Journal of Thermal Analysis and Calorimetry (2018) 133:929–934
https://doi.org/10.1007/s10973-018-7177-z

Thermal decomposition of praseodymium nitrate hexahydrate $Pr(NO_3)_3{\cdot}6H_2O$

P. Melnikov[1] · I. V. Arkhangelsky[1] · V. A. Nascimento[1] · L. C. S. de Oliveira[1] · W. Rodrigues Guimarães[1] · L. Z. Zanoni[1]

Received: 21 December 2017 / Accepted: 4 March 2018 / Published online: 8 March 2018

Abstract
The hexahydrate of praseodymium nitrate hexahydrate $Pr(NO_3)_3{\cdot}6H_2O$ does not show phase transitions in the range of 233–328 K when the compound melts in its own water of crystallization. It is suggested that the thermal decomposition is a complex step-wise process, which involves the condensation of 6 mol of the initial monomer $Pr(NO_3)_3{\cdot}6H_2O$ into a cyclic cluster $6[Pr(NO_3)_3{\cdot}6H_2O]$. This hexamer gradually loses water and nitric acid, and a series of intermediate amorphous oxynitrates is formed. The removal of 68% HNO_3–32% H_2O azeotrope is essentially a continuous process occurring in the liquid phase. At higher temperatures, oxynitrates undergo thermal degradation and lose water, nitrogen dioxide and oxygen, leaving behind normal praseodymium oxide Pr_2O_3. The latter absorbs approximately 1 mol of atomic oxygen from N_2O_5 disproportionation, giving rise to the non-stoichiometric higher oxide $Pr_2O_{3.33}$. All mass losses are satisfactorily accounted for under the proposed scheme of thermal decomposition.

Keywords Rare earth · Praseodymium nitrate hexahydrate · Thermal decomposition

Introduction

Praseodymium nitrate is used as a starting material for the synthesis of organic chelates, whose usage may provide an opportunity to prepare magnetic images contrasts in medicine. One of them is a praseodymium chelate 2-methoxyethyl-Pr-MOE-DO3A, which proved useful to generate in vivo temperature maps with sufficient spatial and temporal resolution [1].

The structure of praseodymium hexahydrate trihydrate [tetraaquatris(nitrato-$\kappa^2$2O,O′)praseodymium(III)dihydrate] is similar to other $[Ln(NO_3)_3(H_2O)_4]{\cdot}2H_2O$ analogues. The asymmetric unit (Fig. 1) consists of a Pr(III) cation, three nitrate anions, and in total six water molecules. The Pr(III) cation is ten-coordinated by the oxygen atoms of three bidentate nitrate anions and four water molecules. Additionally, two lattice water molecules are located in the second coordination shell [2]. This remote water can be expected to be the first to be eliminated during the heat treatment.

The thermal decomposition of $Pr(NO_3)_3{\cdot}6H_2O$ has been the subject of recent research in the study of the genesis and characterization of praseodymium oxide obtained from this hydrate [3]. Although the general conclusions of the study are unobjectionable, it does not explain the mechanism involved, that is, how stoichiometric Pr_6O_{11} with six Pr atoms could have been formed from $PrONO_3$ containing only one Pr atom, without going through the condensation process. Nor does it take into account extensive evidence of hydrolytic processes accompanied by the release of nitric acid during thermolysis of rare earth nitrates [4–13]. So it is possible, in our opinion, that a simpler and more convincing mechanism of thermal decomposition than that proposed by the authors [4] might be suggested. As is known, the decomposition of rare earth nitrates $Ln(NO_3)_3{\cdot}6H_2O$ is not a simple process of water loss. The stability of octahedral complex cations $[Ln(H_2O)_6]^{3+}$ is so high that part of NO_3 groups present in these compounds are eliminated before a complete dehydration is achieved, or at least simultaneously with this process. In this context, the conclusions drawn from the thermal decomposition

✉ P. Melnikov
petrmelnikov@yahoo.com

[1] Federal University of Mato Grosso do Sul, Campo Grande, Mato Grosso do Sul, Brazil

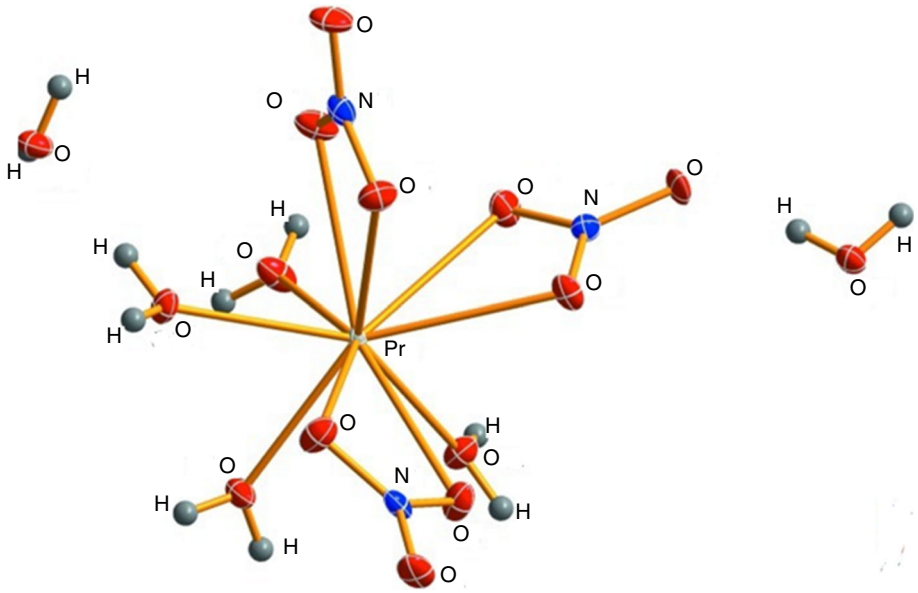

Fig. 1 Structure of $Pr(NO_3)_3{\cdot}6H_2O$. From [2] with modifications

kinetics of the alleged "dehydrated" nitrates [14] are questionable when the compounds are obtained using a method that, in principle, would not have allowed preparing anhydrous salts. The purpose of the present investigation is to revert to the thermolysis of the title hexahydrate offering a different and more realistic scheme of events, especially at the onset of the process.

Materials and methods

The initial reagent employed was praseodymium nitrate trihydrate $Pr(NO_3)_3{\cdot}6H_2O$, of analytical grade purity purchased from Sigma-Aldrich. Direct heating of the commercial reagent up to 1073 K resulted in mass loss of 61.5%, confirming the water number of three (calc. value 62.1%). The reason for a small difference will be discussed below. Thermal gravimetric analysis (TG) and differential scanning calorimetry (DSC) were used to study thermal behavior, in both cases employing a Netsch STA Jupiter 449 C Instrumentation. Test specimens of the starting material (5 mg) were heated in a flux of argon (50 mL min^{-1}, 99.998% purity; oxygen content < 5 ppm) in a 303–773 K temperature range, at a heating rate of 283 K min^{-1}. Platinum microreceptacle was used for heat treatment. Mass losses during heating were analyzed and compared with previously calculated values. Visual observations were carried out in air, using a platinum receptacle, from room temperature to 573 K. The samples were sealed in glass ampoules in a hot condition in order to avoid the impact of water vapors from the air. The evolution of volatiles was measured using a Tensor 27 Bruker FTIR spectrometer attached to the aforementioned Netsch STA Jupiter 449C instrumentation. Temperature of the transport gas line was 513 K. The IR spectra were detected in a 700–4000 cm^{-1} range, taken for 12 s at a frequency accuracy of 1 cm^{-1}. The identification of the spectra was done on the basis of NIST Chemistry WebBook [15].

Results and discussion

As established by visual observations, the title compound melts in its own water of crystallization becoming a greenish transparent liquid at around 348 K. This liquid begins to boil at ~ 398 K, and immediately the odor of gaseous HNO_3 starts to feel. This behavior is characteristic to that of other nitrates hexahydrates [6–8, 12, 13]. Then, at a temperature above 623 K brown vapors of nitrogen dioxide are released.

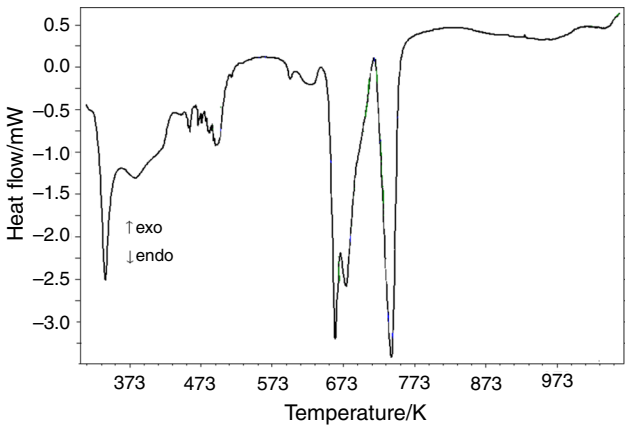

Fig. 2 DSC curve of $Pr(NO_3)_3{\cdot}6H_2O$

The DSC analysis of $Pr(NO_3)_3{\cdot}6H_2O$ is presented in Fig. 2. At lower temperatures, no solid–solid phase transition was found, at least over 233 K. From approximately 311 K on, a series of endothermic effects becomes evident, reflecting the dehydration/decomposition processes. Along with TG pattern, their analysis can be used for a careful interpretation of results.

The representative TG curve of $Pr(NO_3)_3{\cdot}6H_2O$ is shown in Fig. 3. The first mass loss is due to water evaporation after fusion of the original hexahydrate at 310–321 K. This temperature is also confirmed by direct visual observation, when the melt loses gas bubbles and turns into a clear liquid. It is well known that the decomposition onset for the nitrates of trivalent metals is generally below 373 K [16]. In this respect, praseodymium nitrate is not an exception. The first mass loss (1.3%) at 314–455 K corresponds to 2 mol of evaporated water, taking into account the presence of six monomers at the start of decomposition process. Between 455 K and 633 K, the compound loses 26.1% of its mass, corresponding to 15 mol of water and 6 mol of nitric acid. Removal of HNO_3 appears to occur in two subsequent sub-steps. Indeed, this acid, or rather the azeotrope 68% HNO_3–32% H_2O with the boiling point 393 K [17], is detected by the IR sensor during the thermal treatment. Nitric acid is identified by its characteristic absorption bands at 892, 1319, 1508, 1596, 1631 and 1716 cm^{-1}.

The 3D diagram of IR spectrum shown in Fig. 4 gives a general view of absorption at sequential temperatures. Dynamics of HNO_3 removal is illustrated in Fig. 5a.

The next loss of mass (24.6%) occurs between 633 and 723 K, corresponding to the removal of 16 mol of water, 12 mol of nitric dioxide and 6 oxygen. The observation of the characteristic brown color of nitrogen dioxide and the known instability of HNO_3 at high temperatures suggest that the acid in its molecular form is not actually present. It is known that the thermal decomposition of nitric acid

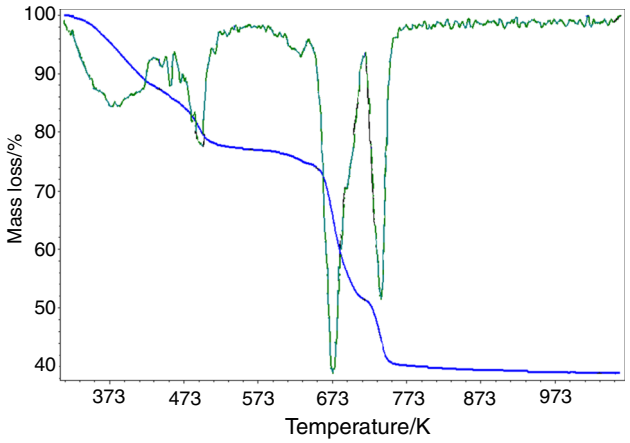

Fig. 3 TG curve of $Pr(NO_3)_3{\cdot}6H_2O$

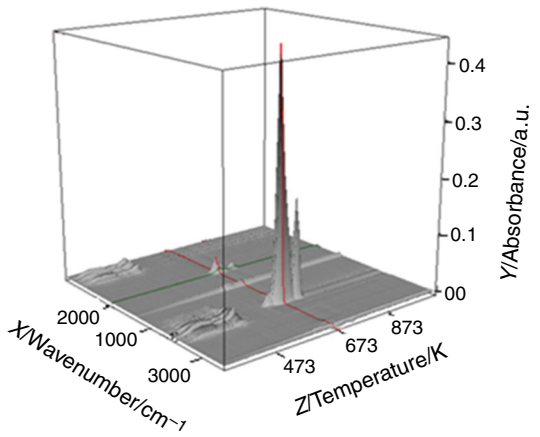

Fig. 4 Temperature-dependent 3D diagram of IR spectra of the $Pr(NO_3)_3{\cdot}6H_2O$ thermal decomposition

represents a reversible endothermic reaction and almost quantitatively proceeds according to the reaction [18]:

$$HNO_3 = NO_2 + 0.5H_2O + 0.25O_2 + 7.8\,\text{kcal mol}^{-1} \quad (1)$$

The presence of nitrogen dioxide at this temperature was further confirmed by the IR spectrum of the volatile products, showing the characteristic bands at 1595 and 1629 cm^{-1} (Fig. 6). Oxygen in principle cannot be registered by this technique due to the lack of changing dipole moment.

This suggests a mechanism that implies the previous formation of N_2O_5 with immediate disproportionation into nitrogen dioxide and atomic oxygen:

$$N_2O_5 = 2NO_2 + O \quad (2)$$

The curves of simultaneous equilibrium of NO, NO_2, N_2O_3 and N_2O_4 show that above 613 K nitrogen dioxide is the only existing phase and HNO_3 practically does not exist [19, 20]. This is evident from the complex dynamics of NO_2 removal illustrated in Fig. 5b. The Gram–Schmidt curve, which describes integrated spectral absorbance of volatile products, corresponds to the TG curve (Fig. 7).

So, at least up to 573 K we do not have the ability to judge about precise compositions, since the mixture is in the liquid state, and the removal of HNO_3 is essentially a continuous process; consequently, solid phases cannot be isolated and identified. It would be reasonable to assume that the pyrolysis curves reflect the presence of various chemical products, not single stoichiometric compounds of definite composition. Unfortunately, amorphous oxynitrate(s) cannot be unambiguously identified by means of IR spectra due to the overlapping bands of nitrate ion and water. Table 1 shows the compositions of the reaction products with expected and experimentally found mass losses at different stages of thermal treatment.

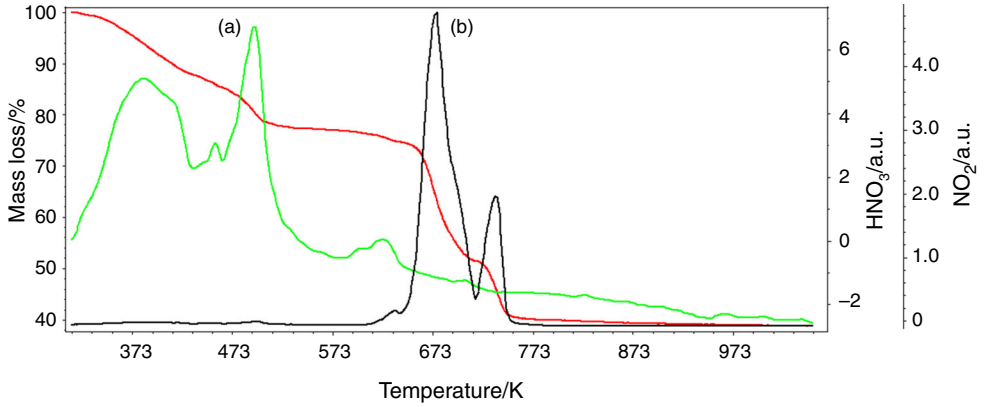

Fig. 5 Dynamics of HNO_3 (a) and NO_2 (b) removal in relation to TG curve

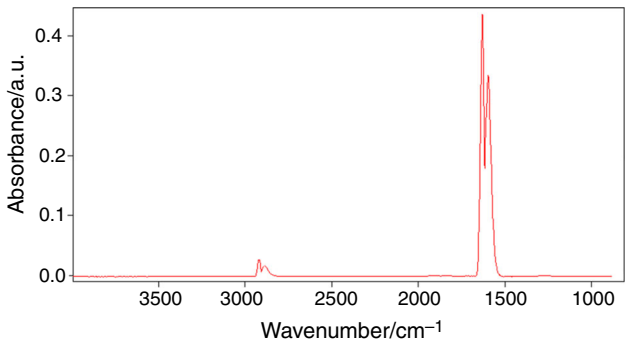

Fig. 6 IR spectrum of nitrogen dioxide detected at 677 K

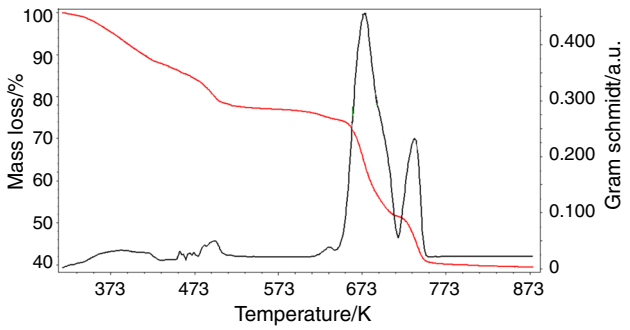

Fig. 7 Gram–Schmidt curve of integrated spectral absorbance in respect of TG

Table 1 Mass losses at different stages of $Pr(NO_3)_3{\cdot}6H_2O$ pyrolysis and compositions of the volatile products in relation to the initial six monomers

	H_2O	HNO_3	NO_2	O	Exp.	Calc.
$[6\ Pr(NO_3)_3]{\cdot}36H_2O$	2				1.3	1.4
$[6\ Pr(NO_3)_3]{\cdot}34H_2O$	15	6			26.1	26.7
$Pr_6(NO_3)_{12}O_3{\cdot}16H_2O$	16		12	6	50.7	50.7
$Pr_6\ O_{9.99}$					61.5	62.1
Total loss (mol)	33	6	12	6		

The small difference between the calculated and experimental mass losses may be explained by the presence of excessive oxygen in the oxidized form of praseodymium oxide.

Actually, after the denitrification has been completed, the only remaining compound is praseodymium oxide. Nevertheless, the X-ray diffraction pattern of the latter shows that the problem is not as simple as it presented itself in an earlier publication [3]. In fact, the diagram given in Fig. 8 allows identifying the final product of thermal decomposition as non-stoichiometric $Pr_2O_{3.33}$ or $Pr_6O_{9.99}$ formed far from equilibrium (published X-ray pattern: ICSD file 647294). This leads to the suggestion that a dynamic oxidation process is taking place that involves internally produced atomic oxygen with the concomitant disproportionation of the oxide. It means, consequently, that a higher non-stoichiometric oxide might be formed as the solid residue. In a previously published research [21], the similar phase could have been obtained exclusively by the use of radiation with an electron beam. These considerations are in accordance with the thermodynamic assessment of the Pr–O system [22]. A notable feature of

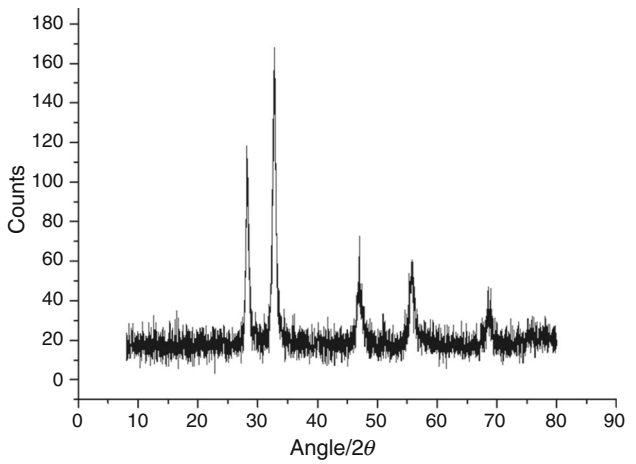

Fig. 8 X-ray powder diagram of the final product of thermal decomposition

this phase diagram is hysteretic behavior whereby different equilibrium oxygen pressures are observed depending on whether an oxidation or reduction path is present. In the present instance, we are definitely dealing with a process of partial oxidation.

In our specific case, the proposed mechanism involves the initial formation of a normal oxide Pr_2O_3 (3) which absorbs about 1 mol of oxygen giving rise to the non-stoichiometric compound (4). The resulting scheme (5) shows that all mass losses are satisfactorily accounted for under the following mechanism of $6[Pr(NO_3)_3{\cdot}6H_2O]$ thermal decomposition:

$$6[Pr(NO_3)_3 \cdot 6H_2O] = Pr_2O_3 + 6HNO_3 + 12NO_2 + 33H_2O + 3O_2 \quad (3)$$

$$3Pr_2O_3 + 0.99O = 3Pr_2O_{3.33} \quad (4)$$

$$6[Pr(NO_3)_3 \cdot 6H_2O] = 3Pr_2O_{3.33} + 6HNO_3 + 12NO_2 + 33H_2O + 5O \quad (5)$$

Indeed, that suggests that at least 6 mol of $Pr(NO_3)_3{\cdot}6H_2O$ is involved in the condensation process. Naturally, like in the instance of $Al(NO_3)_3{\cdot}6H_2O$ [7] or $Sc(NO_3)_3{\cdot}3H_2O$ [9] which contain cations with small ionic radii, we might start considering the condensation of 2 and 4 mol, respectively, but in this case, at the end of the process, we would have to resort to fractional values of stoichiometric coefficients for volatile products, and the need for further condensation up to 6 monomers. This is corroborated by the structures of hexanuclear clusters containing six rare earth atoms [23, 24].

Conclusions

1. The hexahydrate of praseodymium nitrate hexahydrate $Pr(NO_3)_3{\cdot}6H_2O$ does not show phase transitions in the range of 233–328 K when the compound melts in its own water of crystallization.
2. It is suggested that the thermal decomposition is a complex step-wise process, which involves the condensation of 6 mol of the initial monomer $Pr(NO_3)_3{\cdot}6H_2O$ into a cluster $6[Pr(NO_3)_3{\cdot}6H_2O]$.
3. This hexamer gradually loses water and nitric acid, and a series of intermediate amorphous oxynitrates is formed.
4. The removal of 68% HNO_3–32% H_2O azeotrope is essentially a continuous process occurring in the liquid phase.
5. At higher temperatures, partially hydrated oxynitrates undergo thermal degradation and lose water, nitrogen dioxide and oxygen, leaving behind normal praseodymium oxide Pr_2O_3.
6. The latter absorbs approximately 1 mol of atomic oxygen from N_2O_5 disproportionation, giving rise to the non-stoichiometric higher oxide $Pr_2O_{3.33}$.
7. All mass losses are satisfactorily accounted for under the proposed scheme of thermal decomposition.

Acknowledgements The authors are indebted to CNPq and FUNDECT (Brazilian agencies) for financial support.

References

1. Merbach AE, Helm L, Toth E. The chemistry of contrast agents in medical magnetic resonance imaging. 2nd ed. Chichester: Wiley; 2013.
2. Decadt R, Van Der Voort P, Van Driessche I, Van Deun R, Van Hecke K. Redetermination of $[Pr(NO_3)_3(H_2O)_4]{\cdot}2H_2O$. Acta Crystallogr E. 2012;68:i59–60.
3. Hussein GAM, Balboul BAA, A-Warith MA, Othman AGM. Thermal genesis and characterization of praseodymium oxide from praseodymium nitrate hydrate. Thermochim Acta. 2007;369:59–66.
4. Melnikov P, Nascimento VA, Zanoni Consolo LZ. Thermal decomposition of gallium nitrate hydrate and modeling of thermolysis products. J Therm Anal Calorim. 2012;107:1117–21.
5. Melnikov P, Nascimento VA, Zanoni Consolo LZ. Computerized modeling of intermediate compounds formed during thermal decomposition of gadolinium nitrate hydrate. Russ J Phys Chem. 2012;86:1659–63.
6. Melnikov P, Nascimento VA, Consolo LZZ, Silva AF. Mechanism of thermal decomposition of yttrium nitrate hexahydrate $Y(NO_3)_3{\cdot}6H_2O$ and modeling of intermediate oxynitrates. J Therm Anal Calorim. 2013;111:115–9.
7. Melnikov P, Nascimento VA, Arkhangelsky IV, Zanoni Consolo LZ. Thermal decomposition mechanism of aluminum nitrate octahydrate and characterization of intermediate products by the technique of computerized modeling. J Therm Anal Calorim. 2013;111:543–8.
8. Melnikov P, Nascimento VA, Arkhangelsky IV, Zanoni Consolo LZ, de Oliveira LCS. Thermolysis mechanism of chromium nitrate nonahydrate and computerized modeling of intermediate products. J Therm Anal Calorim. 2013;114:1021–7.
9. Melnikov P, Nascimento VA, Arkhangelsky IV, Zanoni Consolo LZ, de Oliveira LCS. Thermal decomposition mechanism of iron (III) nitrate and characterization of intermediate products by the technique of computerized modeling. J Therm Anal Calorim. 2014;115:145–51.
10. Melnikov P, Arkhangelsky IV, Nascimento VA, Silva AF, Zanoni Consolo LZ, de Oliveira LCS, Herrero AS. Thermolysis mechanism of dysprosium hexahydrate nitrate $Dy(NO_3)_3{\cdot}6H_2O$ and modeling of intermediate decomposition products. J Therm Anal Calorim. 2015;122:571–8.
11. Melnikov P, Arkhangelsky IV, Nascimento VA, Silva AF, Zanoni Consolo LZ. Thermolysis mechanism of samarium nitrate hexahydrate. J Therm Anal Calorim. 2014. https://doi.org/10.1007/s10973-014-4067-x.
12. Melnikov P, Nascimento VA, Arkhangelsky IV, Silva AF, Zanoni-Consolo LZ. Thermogravimetric study of the scandium nitrate hexahydrate thermolysis and computer modeling of

intermediate oxynitrates. J Therm Anal Calorim. 2014. https://doi.org/10.1007/s10973-014-4272-7.
13. Melnikov P, Arkhangelsky IV, Nascimento VA, de Oliveira LCS, Silva AF, Zanoni LZ. Thermal analysis of europium nitrate hexahydrate $Eu(NO_3)_3{\cdot}6H_2O$. J Therm Anal Calorim. 2016. https://doi.org/10.1007/s10973-016-6047-9.
14. Strydom CA, Van Vuuren CPJ. The thermal decomposition of lanthanum(III), praseodymium (III) and europium(III) nitrates. Thermochim Acta. 1988;124:277–83.
15. Young DC. Computational chemistry: a practical guide for applying techniques to real-world problems. New York: Wiley; 2001.
16. NIST Chemistry WebBook. NIST Standard Reference Database Number 69. www.http//webbook.nist/chemistry. Accessed 8 May 2016.
17. Huang C-H, editor. Rare earth coordination chemistry. Fundamentals and applications. Singapore: Wiley; 2010.
18. Manelis GB, Nazin GM, Rubtsov YT, Strunin VA. Thermal decomposition and combustion of explosives and propellants. Boca Raton: CRC Press; 2003.
19. Liu Y, Bluck D., Brana-Melero F. Static and dynamic simulation of NO_x absorption tower based on a hybrid-kinetic equilibrium reaction model. In: Eden MR, Siirola JD, Towler GP, editors. Proceedings of the 8th international conference on foundations of computer-aided process design. Amsterdam: Elsevier; 2014.
20. Bibart CH, Ewing GE. Vibrational spectrum of gaseous N_2O_3. J Chem Phys. 1974;61:1293–9.
21. Gasgnier M, Schiffmacher G, Caro P. The formation of rare earth oxides far from equilibrium. J Less Com Met. 1986;116:31–8.
22. Wesley McMurray J. Thermodynamic assessment of the Pr–O system. J Am Ceram Soc. 2016;99:1092–9.
23. Tian H, Guo YN, Zhao L, Tang J, Liu Z. Hexanuclear dysprosium (III) compound incorporating vertex- and edge-sharing Dy3 triangles exhibiting single-molecule-magnet behavior. Inorg Chem. 2011;50:8688–90.
24. Giester G, Unfried P, Zak Z. Synthesis and crystal structure of some new rare earth basic nitrates II: $[Ln_6O(OH)_8(H_2O)_{12}(-NO_3)_6](NO_3)_2{\cdot}xH_2O$, Ln = Sm, Dy, Er; x (Sm) = 6, x(Dy) = 5, x(Er) = 4. J Alloy Compd. 1997;257:175–81.